Heliyon 10 (2024) e37368

Contents lists available at ScienceDirect

Heliyon

journal homepage: www.cell.com/heliyon

Research article

Pseudo-continuous and territorial arterial spin labeling MRI for assessment of cerebral perfusion in moyamoya disease after revascularization: A comparative study with digital subtraction angiography

Juan Li [a], Qinghu Meng [b], Ling Huang [a], Dmytro Pylypenko [c], Hai Zhong [a,*]

[a] Department of Radiology, The Second Hospital of Shandong University, Ji Nan, Shandong Province, 250033, China
[b] Department of Neurosurgery, The Second Hospital of Shandong University, Ji Nan, Shandong Province, 250033, China
[c] MR Research, GE Healthcare, Beijing, 10076, China

ARTICLE INFO

Keywords:
Pseudo-continuous arterial spin labeling
Territory arterial spin labeling
Moyamoya disease
Digital subtraction angiography
Magnetic resonance imaging

ABSTRACT

Purpose: To evaluate if pseudo-continuous arterial spin labeling (pcASL) and territorial ASL (tASL) can assess cerebral perfusion post-revascularization in Moyamoya disease and compare with digital subtraction angiography (DSA) outcomes.
Materials and methods: Patients diagnosed with Moyamoya disease who underwent pcASL using two post-labeling delays (short ASL, 1,525 ms; delayed ASL, 2,525 ms), tASL, and DSA 3 months after surgery at a single institution were retrospectively evaluated. Manual delineation on pcASL cerebral blood flow (CBF) maps covered middle cerebral artery (MCA) territory on both sides, and cerebellum. Normalized CBF (nCBF) was calculated. Revascularization in the MCA territory was evaluated with external carotid angiography and tASL, graded on a three-point scale. Inter-modality agreement was analyzed with weighted κ statistics. Correlation between pcASL-derived nCBF and tASL-measured revascularization, and revascularization grade from direct angiography, was determined. Diagnostic performance of pcASL and tASL was evaluated using DSA as a reference via receiver operating characteristic (ROC) curve analysis.
Results: A total of 32 hemispheres from 31 patients were assessed. On the operated side, sASL and dASL had nCBF values of 1.00 ± 0.30 and 1.31 ± 0.31, respectively. Revascularization area grading showed substantial intermodality agreement (weighted κ = 0.68; 95 % CI: 0.49, 0.87). DSA revascularization moderately correlated with sASL and dASL nCBF values (r = 0.56 and 0.47) and strongly correlated with tASL revascularization area (r = 0.73). ROC analysis revealed that sASL and dASL nCBF values reflected revascularization (area under the curve (AUC) = 0.86 and 0.77) and tASL revascularization area (AUC = 0.91). Combined pcASL and tASL had an AUC of 0.93, comparable to tASL alone, improving diagnostic performance. The diagnostic accuracy of nCBF for sASL was 87.5 %, superior to 75 % for dASL. The diagnostic accuracy of tASL external carotid artery revascularization area was 87.5 %, with sensitivity and specificity of 88 % and 85.7 %, respectively.
Conclusion: The combination of pcASL and tASL outperformed pcASL alone in assessing cerebral perfusion post-Moyamoya disease revascularization.

* Corresponding author. No 247, Beiyuan Street, Jinan, 250033, Shandong Province, China.
E-mail address: 18753107255@163.com (H. Zhong).

https://doi.org/10.1016/j.heliyon.2024.e37368
Received 8 February 2024; Received in revised form 31 August 2024; Accepted 2 September 2024
Available online 3 September 2024
2405-8440/

Abbreviations

AVM	arteriovenous malformation
CBF	cerebral blood flow
CTP	computed tomography perfusion
dASL	delayed arterial spin labeling
DSA	digital subtraction angiography
DSC	dynamic susceptibility contrast
ECA	external carotid artery
ICA	internal carotid artery
MCA	middle cerebral artery
MMD	Moyamoya disease
MRI	magnetic resonance imaging
nCBF	Normalized CBF
pcASL	pseudo-continuous arterial spin labeling
PET	positron emission tomography
PLD	post-labeling delay
sASL	short arterial spin labeling
SNR	signal-to-noise ratio
ss-ASL	super-selective arterial spin labeling
tASL	territorial ASL
VA	vertebral artery

1. Introduction

Moyamoya disease (MMD) is a chronic progressive cerebrovascular occlusion disease of unknown etiology, typically involving the distal ends of bilateral or unilateral internal carotid arteries (ICAs) or the beginnings of the middle and anterior cerebral arteries. It is accompanied by abnormal capillary network formation at the skull base [1,2]. Currently, there is no drug treatment available for MMD. Intracranial and extracranial revascularization surgery is effective in preventing cerebral ischemic reattacks by enhancing intracranial blood flow of the external carotid artery (ECA) and improving cerebral blood flow (CBF). There are three main surgical approaches: direct revascularization, indirect revascularization, and a combination of both [3]. Post-revascularization monitoring is essential to assess bypass patency and changes in CBF status. Traditional perfusion methods, including dynamic susceptibility contrast (DSC) perfusion magnetic resonance imaging (MRI) and computed tomography perfusion (CTP) imaging, are the primary methods for evaluating cerebral perfusion after revascularization [4]. Despite digital subtraction angiography (DSA) being the optimal choice for diagnosing MMD and observing the establishment of collateral circulation, it cannot accurately reflect the perfusion status of the brain parenchyma [5]. These methods also necessitate the use of contrast media, ionizing radiation, and invasive examinations.

Currently, three-dimensional (3D) pseudo-continuous arterial spin labeling (pcASL) is widely used in evaluating MMD, especially in children, due to its non-invasive provision of CBF information without the use of contrast agents. It aids in evaluating collateral vessels and cerebral reactivity, as well as monitoring blood perfusion changes after surgical vascular reconstruction, confirming its effectiveness in postoperative evaluation of MMD [6–8]. Recent studies indicate that ASL-MRI correlates well with DSC-MRI, CTP, positron emission tomography (PET), and single-photon emission tomography in mapping cerebrovascular reserve and CBF [9–12]. However, ASL-MRI is associated with specific limitations. Measured CBF might be underestimated due to long arterial transit times in steno-occlusive arterial segments and collateral pathways. To address this issue, the application of multi-delay or long-label-long-delay algorithms in ASL-MRI could enhance the accuracy of CBF assessments with a satisfactory signal-to-noise ratio (SNR) [13]. Notably, Hara et al. demonstrated that arterial spin labeling using two post-labeling delays (PLDs) can detect PET-measured true CBF and perfusion delay in MMD patients [14]. However, it provides a perfusion image of the entire brain and lacks the ability to illustrate the blood supply area of the bypass vessel.

Territorial arterial spin labeling (tASL) can specifically label a single blood vessel, revealing the corresponding perfusion area, which holds significant clinical value in cerebrovascular occlusive diseases [15–17]. tASL is particularly suitable for patients with MMD, as it can label the ECA of the bypass and show the blood supply area of the reconstructed vessel. This method avoids overlap in DSA and enables a direct observation of brain tissue perfusion, reflecting the postoperative effect of revascularization [18]. Previous studies have compared tASL with DSA, confirming that the two methods have good consistency in evaluating postoperative MMD [19,20]. However, no studies to date have combined pcASL and tASL for postoperative evaluation of MMD and compared them with DSA to assess their diagnostic efficacy. Therefore, the purpose of the present study was to evaluate cerebral perfusion after MMD revascularization by combining pcASL using two PLDs (short arterial spin labeling (sASL), 1,525 ms; delayed arterial spin labeling (dASL), 2,525 ms) and tASL and to conduct a comparative study with DSA.

2. Materials and methods

2.1. Patients

The current study was approved by the institutional review board of The Second Hospital of Shandong University, and all participants provided written informed consent. The study evaluated 31 patients with MMD from July 2020 to October 2023. Patients were included based on the following criteria: 1) MMD confirmed through DSA, with exclusion of vascular stenosis due to atherosclerosis or vasculitis; 2) underwent MMD revascularization; and 3) had MRI and DSA re-examinations three months post-surgery, including 3D pcASL using two PLDs and tASL sequences. The exclusion criteria were: 1) non-MMD patient bypass; 2) lack of DSA during postoperative follow-up; and 3) incomplete MRI scan sequences or significant artifacts affecting postoperative follow-up results. In total, 31 MMD patients were included in the study, with 32 hemispheres analyzed. The demographic data and clinical characteristics of the included patients are detailed in Table 1.

2.2. MRI protocol

All MRI examinations utilized a 3.0 T MRI scanner (GE Signa Pioneer, USA) with a 29-channel head and neck coil. Besides MRA sequences, 3D pseudo-continuous ASL images were acquired using following parameters: repetition times (TR) of 4,649 ms and 5,344 ms, an echo time (TE) of 10.9 ms, a field of view (FOV) of 240 mm × 240 mm, 8 spiral arms each having 512 sampling points, a spatial resolution of 3.79 mm, a section thickness of 4 mm, 3 excitations (NEX), a bandwidth of 62.50 Hz, and a labeling duration of 1,500 ms. Two post-labeling delays (PLDs) of 1,525 ms (sASL) and 2,525 ms (dASL) were used, with corresponding scanning durations of 4 min and 20 s for sASL, and 4 min and 53 s for dASL. The tASL procedure followed a pcASL protocol, using a super-selective approach as described in prior studies [18]. Labeling for TOF MRA was targeted at the ECA, ensuring the center of labeling was away from the ICA and perpendicular to the scan plane. Labeling was placed at the center of the ECA lumen with a radius between 20 and 30 mm, usually set at 30 mm but adjusted when necessary to avoid nearby vessels. This setup included the following parameters: a 240 mm × 240 mm FOV, a slice thickness of 4 mm, a TR of 4,861 ms, a TE of 10.9 ms, 4 spiral arms with 512 sampling points each, a spatial resolution of 5.91 mm, 2 excitations (NEX), a labeling duration of 1,450 ms, a PLD of 2,025 ms, and a scanning time of 1 min and 20 s. Structural imaging was performed using 3D T1 Bravo, with parameters including a 240 mm × 240 mm FOV, an isotropic resolution of 1.0 mm, a TR of 7.3 ms, a TE of 2.7 ms, and 1 excitation (NEX). The GE Advantage Workstation 4.6 was used to combine and color-code the pcASL and tASL images with the 3D T1 brain volume images.

2.3. DSA protocol

Using a DSA system (Innova IGS 630, GE Healthcare), cerebral angiography was performed. After selective catheterization and intra-arterial injection of a nonionic monomeric iodine contrast medium, anteroposterior and lateral projection images were obtained for each subject. The procedure involved the use of a 5-F catheter in the bilateral internal carotid arteries (ICAs), external carotid arteries (ECAs), and the dominant vertebral artery (VA). Iodixanol-330 (GE Healthcare) served as the contrast medium, which was injected at a rate of 3 mL/s and a similar volume across all cases.

2.4. Image analysis

Image post-processing and analysis were carried out using the GE post-processing workstation ADW 4.6. The vendor-provided

Table 1
Study sample characteristics.

Characteristic	Value
No. of patient	31
Age (y), mean (range)	44 (8–62)
M:F	11:20
Initial clinical presentation, number	
Ischemia type	28
Hemorrhage type	3
Surgery methods, number	
Direct revascularization	13
Indirect revascularization	5
Combined surgery	14
No. of bypass hemispheres	32
Bypass side	
Right	19
Left	11
Bilateral	1
Follow-up interval after bypass surgery (mo) mean (range)	10 (4–48)
Interval between postoperative DSA and MRI Imaging (d) mean (range)	1.5 (1–3)

software Functool was used to analyze pcASL and tASL, generating pseudo-color images of cerebral blood flow (CBF) distribution. Two experienced neuroradiologists (J.L. with nine years and L.H. with 16 years of clinical experience) independently drew the largest possible regions of interest (ROIs) over the bilateral middle cerebral artery (MCA) territory on the pcASL CBF maps at the centrum semi-ovale level. The ROI was defined as the cortex and subcortical white matter supplied by the MCA leptomeningeal arteries. Each ROI's mean signal intensity value represented the apparent CBF in the MCA territory (CBF_{MCA}), measured in mL/100 g/min, directly obtained from each PLD. These values were influenced by the PLD used. Additional ROIs were drawn on the right and left cerebellar hemispheres to normalize the CBF. The apparent CBF values for the cerebellum (CBF_{Cbll}) were defined as the average of the right and left CBF_{Cbll}. The ROI size was set at a minimum of 2,000 mm^2 for the MCA territory and 350 mm^2 for the cerebellum. Normalized CBF (nCBF) was calculated with the equation: $nCBF = CBF_{MCA}/CBF_{Cbll}$.

The areas of revascularization in each modality were evaluated by two neuroradiologists (J.L. with nine years and Q.H.M. with over 20 years of clinical experience) in consensus. They reviewed all tASL images first, followed by the DSA images on the same day, while being blinded to each modality's findings. The revascularization area was scored using a modified Matsushima grade as follows: 1 for an area less than one-third of the MCA territory (Matsushima grade C), 2 for an area between one-third and two-thirds of the MCA territory (Matsushima grade B), and 3 for an area more than two-thirds of the MCA territory (Matsushima grade A).

2.5. *Statistical analysis*

All statistical analyses were conducted using the Statistical Program for Social Sciences (SPSS) software, version 22.0. Data were expressed as mean ± standard deviation (SD). Inter-observer consistency of sASL- and dASL-derived CBF measurements was assessed using the intra-class correlation coefficient (ICC), with values above 0.75 indicating good repeatability. The correlation between sASL, dASL nCBF values, tASL ECA reconstruction area, and DSA was analyzed using Kendall's tau-b correlation. Inter-modality and inter-reader agreement values were compared using the weighted κ concordance index, interpreted as follows: slight ($\kappa = 0$–0.20), fair ($\kappa =$ 0.21–0.40), moderate ($\kappa = 0.41$–0.60), substantial ($\kappa = 0.61$–0.80), and almost perfect agreement ($\kappa = 0.81$–1) [21]. The diagnostic efficacy of sASL, dASL, and tASL in MMD revascularization was evaluated using the receiver operating characteristic (ROC) curve, with a dichotomized DSA collateral grading as the reference standard. A P value of <0.05 was considered statistically significant.

3. Results

The present study included 31 patients (mean age, 44 years ±12 [SD]; 20 women) who underwent reconstruction surgery and a total of 32 hemispheres. The clinical characteristics of the 31 patients in the study sample are summarized in Table 1. Further analyses were conducted for the bypassed hemispheres ($n = 32$). All patients underwent intracranial and extracranial vascular reconstruction surgery, including 14 patients who underwent superficial temporal artery-MCA bypass combined with temporalis application and cerebral dura mater turnover, 13 patients who underwent unilateral superficial temporal artery-MCA bypass, four patients who underwent temporalis application and cerebral dura mater turnover, and one child who underwent contralateral surgery 7 months later. Intraoperative fluorescence staining confirmed bypass anastomosis patency in all patients. A total of 31 patients were enrolled, 32 cerebral hemisphere operations were performed, and the follow-up time for unilateral operations ranged from 4 to 48 months, with a median follow-up time of 10 months. After 3 months of follow-up, DSA showed that 93 % (25/27) of the cerebral hemispheres had patency in the direct bypass, and two patients showed direct bypass vessel occlusion.

3.1. *CBF values after cerebral revascularization on sASL and dASL*

ICC analysis confirmed excellent inter-observer agreement between two independent neuroradiologists, with a high ICC value of 0.980 (95 % confidence interval (CI): 0.970–0.986, $P < 0.05$). The mean apparent CBF values on the operated side for sASL and dASL were 44.47 ± 17.39 (mL/100 g/min) and 54.02 ± 14.27 (mL/100 g/min), respectively. The mean apparent CBF values on the contralateral side for sASL and dASL were 47.58 ± 15.67 (mL/100 g/min) and 54.91 ± 14.06 (mL/100 g/min), respectively. The nCBF values for sASL and dASL were 1.00 ± 0.30 and 1.31 ± 0.31, respectively.

Table 2
Revascularization area grading with DSA and territorial ASL ipsilateral external carotid artery MRI.

DSA	tASL Imaging			
	Grade 1	Grade 2	Grade 3	Total
Grade 1	6	1	0	7
Grade 2	3	6	2	11
Grade 3	0	3	11	14
Total	9	10	13	32

Note: Revascularization area grading: 1, area less than one-third of the middle cerebral artery (MCA) territory; 2, area between one-third and two-thirds of the MCA territory; 3, area more than two-thirds of the MCA territory. Weighted $\kappa = 0.68$ (95 % confidence interval: 0.49–0.87, $P < 0.01$). DSA = digital subtraction angiography, tASL = territorial arterial spin labeling.

3.2. Postoperative revascularization area assessment

The inter-reader agreement was excellent with a weighted κ of 0.91 (95 % CI: 0.85–0.94, $P < 0.01$). The intermodality agreement of revascularization area grading is shown in Table 2, Fig. 1. The revascularization area agreement between DSA and tASL images was substantial with a weighted κ of 0.68 (95 % CI: 0.49–0.87, $P < 0.01$).

3.3. Correlation between sASL, dASL nCBF, tASL, and DSA

DSA revascularization was moderately correlated with sASL nCBF (correlation coefficient $r = 0.56$), weakly correlated with dASL nCBF (correlation coefficient $r = 0.47$), and strongly correlated with tASL revascularization area (correlation coefficient $r = 0.73$). The correlation data are presented in Table 3.

3.4. Diagnostic performance of sASL, dASL, and tASL MRI

DSA was categorized into grades 2 and 3 for well-reconstructed blood flow and grade 1 for slightly poorly reconstructed blood flow, serving as a reference for the diagnostic performance of pcASL and tASL. The area under the curve (AUC) in discriminating between the groups with well-reconstructed and slightly poorly reconstructed blood flows was higher for tASL (AUC = 0.91) than for sASL and dASL (AUC = 0.86, 0.78, respectively; Table 4, Fig. 2). The AUC value for the combined tASL and pcASL diagnosis was higher than that for pcASL alone (AUC = 0.93). The diagnostic performance of pcASL was enhanced when combined with tASL. Table 5 shows the diagnostic performance of sASL, dASL, and tASL imaging in the ipsilateral ECA territory for the presence of collateral flow. The diagnostic accuracy of sASL was 87.5 %, which was comparable to that of tASL but superior to the 75 % for dASL. Furthermore, sASL sensitivity and specificity values for diagnosing revascularization were 88 % and 85.7 %, respectively, which were superior to 72 % and 85.7 % for dASL.

4. Discussion

The present study assessed the suitability of pcASL and tASL imaging for monitoring the revascularization area following bypass surgery in MMD patients. The findings revealed substantial agreement between tASL imaging and DSA (weighted κ = 0.68; 95 % CI: 0.49, 0.87). In addition, sASL and dASL exhibited moderate or weak correlations with DSA, while tASL demonstrated a strong correlation. tASL imaging also showed an excellent diagnostic performance in determining the quality of reconstructed blood flow in the

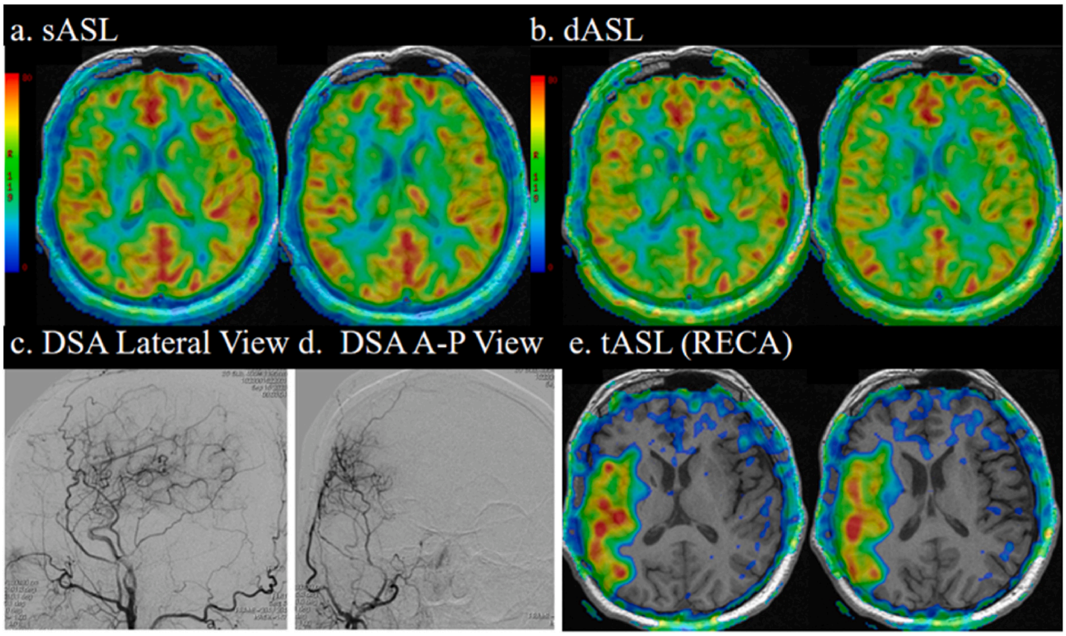

Fig. 1. Images of 42-year-old man diagnosed with right unilateral Moyamoya disease. Patient underwent combined direct and indirect bypass surgery on the right side, as well as digital subtraction angiography (DSA), short arterial spin labeling (sASL), delayed arterial spin labeling (dASL), and territorial arterial spin labeling (tASL) 12 months after surgery. (a, b) Postoperative sASL and dASL showed the same perfusion in the left and right cerebral hemispheres. (c. d) Postoperative lateral (c) and anteroposterior (d) right external carotid arteriograms show areas of revascularization in right MCA territory (more than two-thirds of MCA territory). (e) Right external carotid artery (ECA) territory ASL also depicts supplying territory in right MCA territory (more than two-thirds of MCA territory).

Table 3
Correlation analysis between sASL, dASL, tASL, and DSA.

Correlation	Correlation coefficient	P value
sASL and DSA	0.56	<0.001
dASL and DSA	0.47	0.001
tASL and DSA	0.73	<0.001

Note: sASL = short arterial spin labeling, dASL = delayed arterial spin labeling, tASL = territorial arterial spin labeling, DSA = digital subtraction angiography.

Table 4
Diagnostic performance of sASL, dASL, tASL, and pcASL + tASL in revascularization flow identification.

Diagnostic performance	AUC	95 % CI	P value
sASL	0.86	0.67–1.00	<0.01
dASL	0.78	0.60–0.95	0.03
tASL	0.91	0.80–1.00	<0.01
pcASL + tASL (combined)	0.93	0.81–1.00	<0.01

Note: sASL = short arterial spin labeling, dASL = delayed arterial spin labeling, tASL = territorial arterial spin labeling, pcASL + tASL (combined) = short arterial spin labeling + delayed arterial spin labeling + territorial arterial spin labeling.

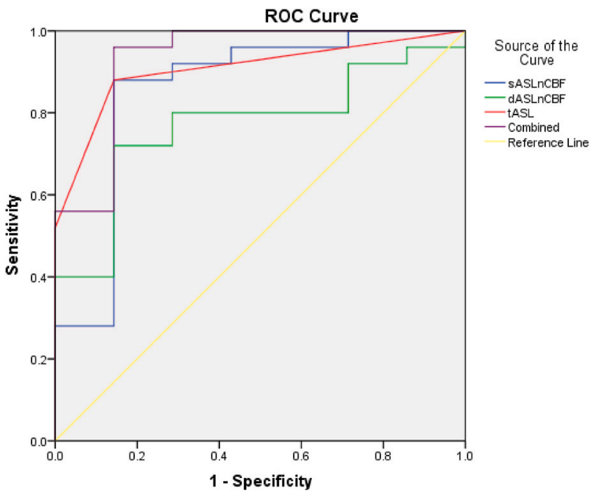

Fig. 2. ROC curve shows sensitivity and specificity values for predicting bypass revascularization outcomes for sASL nCBF, dASL nCBF, and tASL. Predictive value of good prognosis in postoperative tASL (AUC = 0.91, 95 % CI: 0.80–1.00, P < 0.01) was higher than that in sASL nCBF and dASL nCBF. Combined sASL, dASL, and tASL had highest diagnostic performance (AUC = 0.93.95 % CI: 0.81–1.00, P < 0.01).

Table 5
Diagnostic performance of tASL and pcASL imaging in identification of revascularization flow using DSA as a reference test.

	Sensitivity (%)	Specificity (%)	Positive Predictive Value (%)	Negative Predictive Value (%)	Accuracy (%)
sASL	88 %	85.7 %	95.65 %	66.67 %	87.5 %
dASL	72 %	85.7 %	94.74 %	46.15 %	75 %
tASL	88 %	85.7 %	95.65 %	66.67 %	87.5 %

Note: sASL = short arterial spin labeling, dASL = delayed arterial spin labeling, tASL = territorial arterial spin labeling, DSA = digital subtraction angiography.

ipsilateral ECA, surpassing the performance of sASL and dASL, as evident from the higher AUC of 0.91. The combined use of pcASL and tASL yielded the highest diagnostic performance with an AUC of 0.93.

Some prior studies have highlighted the consistent perfusion range between tASL and DSA in the ICA and VA [22,23]. Hwang et al. reported high sensitivity (92 %) and specificity (83 %) for super-selective arterial spin labeling (ss-ASL) and DSA in assessing ECA postoperative blood supply following MMD revascularization, with substantial intermodality agreement in revascularization area grading [19]. Yuan et al. demonstrated consistency in blood flow between ss-ASL and DSA, emphasizing the challenges due to low preoperative collateral blood flow in ECA affecting ss-ASL sensitivity and specificity [20]. The present results align with these studies, suggesting good agreement between tASL and DSA in assessing ECA blood supply after MMD.

However, assessing the ECA bypass alone may not suffice. Simultaneous observation of ICA and VA blood flow, as well as monitoring MMD progression, is crucial. We found that with the extension of follow-up time, the internal carotid artery blood flow for most patients may become thinner, and the moyamoya vessels may diminish. This may be due to the further progression of moyamoya disease or the improvement of brain tissue blood supply with reduced compensatory blood flow demand (decreased blood flow and negative remodeling, leading to diminished blood vessels). Similar changes can occur in the vertebrobasilar arteries. However, a small number of patients had no significant changes in the internal carotid artery or vertebral artery. Since tASL provides qualitative rather than quantitative CBF measurements, conducting whole-brain perfusion imaging and quantitative measurements concurrently is imperative. Previous studies evaluating collateral circulation in MMD patients revealed moderate to strong agreement between ASL and DSA consensus readings, demonstrating ASL's high sensitivity and specificity in identifying collateral circulation [24,25].

The conventional use of pcASL involves a single PLD, representing the time between blood labeling and 3D data acquisition. However, given ASL's sensitivity to arrival time, it may underestimate CBF in regions with delayed arterial arrival times in MMD patients. To address this, the present study employed two PLDs, including sASL (1,525 ms) and dASL (2,525 ms). sASL offered a better SNR, while dASL captured CBF in the delayed perfusion area of MMD. The present study demonstrated a correlation drop in dASL compared to sASL, possibly due to the fundamental trade-off between short and long delays described by Alsop et al., where short delays may compromise delivery of labeled blood water to tissue, and long delays result in strong T1 decay and reduced SNR [26]. Our results indicate that the apparent CBF values obtained from sASL and dASL provide complementary information on cerebral perfusion under different PLD conditions. The differences in CBF values highlight the impact of PLD on the measurement, reflecting variations in blood arrival times and signal decay.

The present study observed postoperative blood flow on the operated side to be equal to or higher than contralateral blood flow, indicating positive postoperative effects. Although some patients exhibited underperfusion areas in sASL, dASL complemented by capturing delayed perfusion presented a more comprehensive picture. Cerebellar blood flow remained relatively stable and blood flow in the MCA was compared to that in the cerebellum for normalization. Many studies have used cerebellar blood flow as a reference standard [8,27,28]. Yun et al. showed that although different methods were used, the nCBF value on the anastomotic side often increased with prolonged follow-up time [29]. While a stable hemodynamic state is generally expected 6 months after surgery, two cases 4 months post-surgery did not reveal abundant bypass vessels or new vessels, affecting tASL's ability to detect ECA blood flow.

Compared to other methods, a distinctive feature of tASL imaging is that it can display the perfusion of a single vessel—not only the revascularization of bypass vessels but also the blood supply of the internal carotid artery and vertebrobasilar artery. tASL can determine the responsible blood vessels in patients with ischemic stroke, especially in the watershed area. Hartkamp et al. found that using the standard perfusion territory atlas and MRA alone could not accurately determine the responsible blood vessels [30]. tASL can also assess collateral circulation in stenotic or occlusive diseases of the major arteries, and for patients with complex cerebrovascular occlusions, tASL plays a more prominent role. Even when extracranial stenoses and circle of Willis anatomies are similar, the perfusion patterns can differ [31]. Additionally, tASL can identify the supplying arteries in patients with arteriovenous malformations (AVM). Togao et al. used ss-ASL based four-dimensional (4D) MRA to identify the supplying arteries of AVM, improving the accuracy of diagnosing the supplying arteries with the assistance of ss-ASL [32]. Moreover, tASL imaging offers the advantage of providing cross-sectional images, allowing for precise localization of the perfusion area through fusion with anatomical images (3D T1). This facilitates direct observation of brain tissue blood supply, in contrast to DSA's projected images, which can only be inferred. Combining whole-brain perfusion and regional perfusion imaging enhances diagnostic performance, particularly in pediatric cases, owing to tASL's non-invasive and reproducible nature.

Several limitations exist in the present study. The sample size was limited, warranting future studies with expanded cohorts. Follow-up times varied, potentially impacting postoperative results. Moreover, the study focused solely on changes in cerebral perfusion post-MMD revascularization without comparing preoperative cerebral perfusion. This aspect will be explored in subsequent research.

In conclusion, the present study demonstrated that pcASL with two PLDs allowed for quantitative evaluation of CBF changes post-MMD surgery. When combined with tASL, which provides qualitative assessment of ECA reconstructed blood flow, a comprehensive evaluation of post-surgery reconstruction effects was achieved, incorporating both quantitative and qualitative aspects.

Data availability statement

Data will be available on request.

Ethics statement

This study was conducted in accordance with the ethical regulations of the Declaration of Helsinki. The research was approved by the Ethics Committee of The Second Hospital of Shandong University (NO: KYLL2024420).

CRediT authorship contribution statement

Juan Li: Writing – original draft, Data curation. **Qinghu Meng:** Methodology, Data curation. **Ling Huang:** Visualization, Methodology, Formal analysis, Data curation. **Dmytro Pylypenko:** Writing – review & editing, Visualization. **Hai Zhong:** Writing – review & editing, Supervision, Methodology, Conceptualization.

Declaration of competing interest

The authors declare that they have no known competing financial interests or personal relationships that could have appeared to influence the work reported in this paper.

Acknowledgements

We would like to express our great appreciation to the editor and anonymous reviewers for their comments, which helped us to improve the quality of our paper. We thank International Science Editing (http://www.internationalscienceediting.com) for editing this manuscript.

References

[1] M. Ihara, Y. Yamamoto, Y. Hattori, et al., Moyamoya disease: diagnosis and interventions, Lancet Neurol. 21 (8) (Aug 2022) 747–758, https://doi.org/10.1016/S1474-4422(22)00165-X.
[2] J.S. Kim, Moyamoya disease: epidemiology, clinical features, and diagnosis, J. Stroke . 18 (1) (Jan 2016) 2–11, https://doi.org/10.5853/jos.2015.01627.
[3] V.N. Nguyen, M. Motiwala, T. Elarjani, et al., Direct, indirect, and combined extracranial-to-intracranial bypass for adult moyamoya disease: an updated systematic review and meta-analysis, Stroke 53 (12) (Dec 2022) 3572–3582, https://doi.org/10.1161/STROKEAHA.122.039584.
[4] L. Du, H. Jiang, J. Li, T. Duan, C. Zhou, F. Yan, Imaging methods for surgical revascularization in patients with moyamoya disease: an updated review, Neurosurg. Rev. 45 (1) (Feb 2022) 343–356, https://doi.org/10.1007/s10143-021-01596-0.
[5] X. Zhang, W. Xiao, Q. Zhang, et al., Progression in moyamoya disease: clinical features, neuroimaging evaluation, and treatment, Curr. Neuropharmacol. 20 (2) (2022) 292–308, https://doi.org/10.2174/1570159X19666210716114016.
[6] G. Zaharchuk, H.M. Do, M.P. Marks, J. Rosenberg, M.E. Moseley, G.K. Steinberg, Arterial spin-labeling MRI can identify the presence and intensity of collateral perfusion in patients with moyamoya disease, Stroke 42 (9) (Sep 2011) 2485–2491, https://doi.org/10.1161/STROKEAHA.111.616466.
[7] V.L. Rao, L.M. Prolo, J.D. Santoro, et al., Acetazolamide-challenged arterial spin labeling detects augmented cerebrovascular reserve after surgery for moyamoya, Stroke 53 (4) (Apr 2022) 1354–1362, https://doi.org/10.1161/STROKEAHA.121.036616.
[8] S. Lee, T.J. Yun, R.E. Yoo, et al., Monitoring cerebral perfusion changes after revascularization in patients with moyamoya disease by using arterial spin-labeling MR imaging, Radiology 288 (2) (Aug 2018) 565–572, https://doi.org/10.1148/radiol.2018170509.
[9] R. Wang, S. Yu, J.R. Alger, et al., Multi-delay arterial spin labeling perfusion MRI in moyamoya disease–comparison with CT perfusion imaging, Eur. Radiol. 24 (5) (May 2014) 1135–1144, https://doi.org/10.1007/s00330-014-3098-9.
[10] H. Zhang, M. Lu, S. Liu, et al., The value of 3D pseudo-continuousarterial spin labeling perfusion imaging in moyamoya disease-Comparison with dynamic susceptibility contrast perfusion imaging, Front. Neurosci. 16 (Aug 2022) 944246, https://doi.org/10.3389/fnins.2022.944246.
[11] S.B. Lee, S. Lee, Y.J. Cho, Y.H. Choi, J.E. Cheon, W.S. Kim, Monitoring cerebral perfusion changes using arterial spin-labeling perfusion MRI after indirect revascularization in children with moyamoya disease, Korean, J. Radiol. 22 (9) (Sep 2021) 1537–1546, https://doi.org/10.3348/kjr.2020.1464.
[12] R. Goetti, G. Warnock, F.P. Kuhn, et al., Quantitative cerebral perfusion imaging in children and young adults with Moyamoya disease: comparison of arterial spin-labeling-MRI and H(2)[(15)O]-PET, AJNR. Am. J. Neuroradiol. 35 (5) (May 2014) 1022–1028, https://doi.org/10.3174/ajnr.A3799.
[13] A.P. Fan, J. Guo, M.M. Khalighi, et al., Long-delay arterial spin labeling provides more accurate cerebral blood flow measurements in moyamoya patients: a simultaneous positron emission tomography/MRI study, Stroke 48 (9) (Sep 2017) 2441–2449, https://doi.org/10.1161/STROKEAHA.117.017773.
[14] S. Hara, Y. Tanaka, Y. Ueda, et al., Noninvasive evaluation of CBF and perfusion delay of moyamoya disease using arterial spin-labeling MRI with multiple postlabeling delays: comparison with 15O-gas PET and DSC-MRI, AJNR. Am. J. Neuroradiol. 38 (4) (Apr 2017) 696–702, https://doi.org/10.3174/ajnr.A5068.
[15] P.J. van Laar, J. van der Grond, J.P. Bremmer, C.J. Klijn, J. Hendrikse, Assessment of the contribution of the external carotid artery to brain perfusion in patients with internal carotid artery occlusion, Stroke 39 (11) (Nov 2008) 3003–3008, https://doi.org/10.1161/STROKEAHA.108.514265.
[16] X. Wang, W. Dou, D. Dong, et al., Can 3D pseudo-continuous territorial arterial spin labeling effectively diagnose patients with recanalization of unilateral middle cerebral artery stenosis? J. Magn. Reson. Imag. 54 (1) (Jul 2021) 175–183, https://doi.org/10.1002/jmri.27560.
[17] T. Lin, Z. Lai, Y. Lv, et al., Effective collateral circulation may indicate improved perfusion territory restoration after carotid endarterectomy, Eur. Radiol. 28 (2) (Feb 2018) 727–735, https://doi.org/10.1007/s00330-017-5020-8.
[18] J. Yuan, J. Qu, D. Zhang, et al., Cerebral perfusion territory changes after direct revascularization surgery in moyamoya disease: a territory arterial spin labeling study, World. Neurosurg. 122 (Feb 2019) e1128–e1136, https://doi.org/10.1016/j.wneu.2018.11.002.
[19] I. Hwang, W.S. Cho, R.E. Yoo, et al., Revascularization evaluation in adult-onset moyamoya disease after bypass surgery: superselective arterial spin labeling perfusion MRI compared with digital subtraction angiography, Radiology 297 (3) (Dec 2020) 630–637, https://doi.org/10.1148/radiol.2020201448.
[20] J. Yuan, J. Qu, Z. Lv, et al., Assessment of blood supply of the external carotid artery in moyamoya disease using super-selective pseudo-continuous arterial spin labeling technique, Eur. Radiol. 31 (12) (Dec 2021) 9287–9295, https://doi.org/10.1007/s00330-021-07893-y.
[21] J.R. Landis, G.G. Koch, The measurement of observer agreement for categorical data, Biometrics 33 (1) (Mar 1977) 159–174.
[22] A.P. Kansagra, E.C. Wong, Mapping of vertebral artery perfusion territories using arterial spin labeling MRI, J. Magn. Reson. Imag. 28 (3) (Sep 2008) 762–766, https://doi.org/10.1002/jmri.21462.
[23] S.M. Chng, E.T. Petersen, I. Zimine, Y.Y. Sitoh, C.C. Lim, X. Golay, Territorial arterial spin labeling in the assessment of collateral circulation: comparison with digital subtraction angiography, Stroke 39 (12) (Dec 2008) 3248–3254, https://doi.org/10.1161/STROKEAHA.108.520593.
[24] G. Zaharchuk, H.M. Do, M.P. Marks, J. Rosenberg, M.E. Moseley, G.K. Steinberg, Arterial spin-labeling MRI can identify the presence and intensity of collateral perfusion in patients with moyamoya disease, Stroke 42 (9) (Sep 2011) 2485–2491, https://doi.org/10.1161/STROKEAHA.111.616466.
[25] S.S. Lang, A.M. Tucker, C. Schreiber, et al., Arterial spin labeling as an ancillary assessment to postoperative conventional angiogram in pediatric moyamoya disease, J. Neurosurg. Pediatr. 29 (1) (Oct 2021) 40–47, https://doi.org/10.3171/2021.7.PEDS21302.
[26] D.C. Alsop, J.A. Detre, X. Golay, et al., Recommended implementation of arterial spin-labeled perfusion MRI for clinical applications: a consensus of the ISMRM perfusion study group and the European consortium for ASL in dementia, Magn. Reson. Med. 73 (1) (Jan 2015) 102–116, https://doi.org/10.1002/mrm.25197.
[27] J.Y. Ha, Y.H. Choi, S. Lee, et al., Arterial spin labeling MRI for quantitative assessment of cerebral perfusion before and after cerebral revascularization in children with moyamoya disease, Korean, J. Radiol. 20 (6) (Jun 2019) 985–996, https://doi.org/10.3348/kjr.2018.0651.
[28] H. Järnum, E.G. Steffensen, L. Knutsson, et al., Perfusion MRI of brain tumours: a comparative study of pseudo-continuous arterial spin labelling and dynamic susceptibility contrast imaging, Neuroradiology 52 (4) (Apr 2010) 307–317, https://doi.org/10.1007/s00234-009-0616-6.
[29] T.J. Yun, J.C. Paeng, C.H. Sohn, et al., Monitoring cerebrovascular reactivity through the use of arterial spin labeling in patients with moyamoya disease, Radiology 278 (1) (Jan 2016) 205–213, https://doi.org/10.1148/radiol.2015141865.
[30] N.S. Hartkamp, J. Hendrikse, L.J. De Cocker, G.J. de Borst, L.J. Kappelle, R.P. Bokkers, Misinterpretation of ischaemic infarct location in relationship to the cerebrovascular territories, J. Neurol. Neurosurg. Psychiatry 87 (10) (Oct 2016) 1084–1090, https://doi.org/10.1136/jnnp-2015-312906.
[31] V. Richter, M. Helle, M.J. van Osch, et al., MR imaging of individual perfusion reorganization using superselective pseudocontinuous arterial spin-labeling in patients with complex extracranial steno-occlusive disease, AJNR. Am. J. Neuroradiol. 38 (4) (Apr 2017) 703–711, https://doi.org/10.3174/ajnr.A5090.
[32] O. Togao, M. Obara, M. Helle, et al., Vessel-selective 4D-MR angiography using super-selective pseudo-continuous arterial spin labeling may be a useful tool for assessing brain AVM hemodynamics, Eur. Radiol. 30 (12) (Dec 2020) 6452–6463, https://doi.org/10.1007/s00330-020-07057-4.